

# Laser application for precision measurements

By H.J. Tiziani<sup>1)</sup>

## 1. Introduction

The laser was introduced 1960 and the holographic interferometry 1965. At first, holography and holographic interferometry were thought to be the answer to most of the problems in optical metrology especially for deformation and vibration analysis. The lack of success was primarily attributed to the quantitative analysis of holographic data. Even today, more than 20 years later, there is not yet a general simple method available, that can be used reliably for the quantitative analysis of holographic fringe patterns to obtain information on deformation and strain as well as on displacements and vibrations of arbitrary 3 D-objects. However, a number of techniques and systems based on techniques used in interferometry have been developed for specific applications. It seems that a combination of different methods can lead to powerful solutions to problems in industry. Furthermore speckle photography and especially speckle interferometry are becoming useful tools in metrology. Shape and defect analysis are becoming important in modern manufacturing; new sensors together with robotics and robotic vision will be developed.

Interferometry and holographic interferometry are becoming useful tools for precision measurements in research and industrial applications. Computer analysis is increasingly important in interferometry. The use of solid state detector arrays, image memory boards together with microprocessors and computers for the extraction of the information from the interferograms and high resolution graphic boards find important applications in optical metrology. Much more information can be extracted from the interferograms leading to higher sensitivities and accuracies.

Automated quantitative evaluation of interferograms requires accurate interference phase measurements, independent of fringe position and intensity variations superposed onto the interferograms. In many interferometric arrangements, phase shifting or heterodyne techniques have been introduced for automatic fringe analysis.

In the phase shifting technique or quasi-heterodyne technique the relative phase is changed continuously or stepwise, using at least three phase shifts of 90 or 120 degrees. The phase of the interference patterns can then be computed from the different measured intensity values. The phase shifting technique is very appropriate for digital processing and TV techniques. Interferometry and two reference beam holography together with video electronic processing lead to a sensitivity of 1/100 of a fringe at any point of the fringe pattern in the TV image. In heterodyne methods the relative phase increases linearly in time and the reference phase is measured electronically at the beat frequency of the reconstructed wavefields. Heterodyne holographic interferometry offers high spatial resolution and interpolation up to 1/1000 of a fringe. It requires, however, sophisticated electronic equipment and mechanical scanning of the fringe pattern [9].

For engineering applications real time techniques in interferometry, holographic interferometry as well as for speckle applications are desired. Thermoplastic material is used frequently for the hologram storage in engineering applications. Photorefractive crystals are found to be useful for real time holography and speckle applications.

## 2. Interferometric testing

Solid state detector arrays, and microprocessors are mostly responsible for the progress in interferometric testing being made during the last few years. Digital interferometry provides means for obtaining very precise measurements at rapid rates.

For the fringe analysis many different methods are applied. They can be classified into static and dynamic methods. In static methods a tilt is introduced to avoid closed fringes. The fringe centers can be found manually and by using a digitizing tablet as well as by using video- and image processing techniques. Furthermore, phase detection technique in the spatial domain using Fourier transformation [1,14] or Fourier analysis in connection with video technique can be used.

For dynamic algorithm the relative phase between the reference beam and the test beam in an interferometer is varied at constant, controlled rate or in steps of 90 or 120 degrees for instance [2].

Dynamic techniques are:

- phase shifting in three or four steps or continuously
- heterodyne technique
- phase locked technique

The intensity of the interference pattern can be written as

$$I(x,y) = I_0(x,y) \left\{ 1 + b(x,y) \cos [\phi(x,y) + \Delta] \right\} \quad (1)$$

where  $I_0$  is the average intensity at each detector point,  $b$  is the modulation of the fringe pattern.

$\phi(x,y) = \frac{2\pi}{\lambda} W(x,y)$  is the phase distribution of the wavefront  $W(x,y)$  across the interference pattern to be measured

and

$\Delta$  the deliberately introduced phase shift.

The interference pattern can be recorded by a solid state detector array. For the phase shifting technique at least three patterns with the appropriate phase shifts need to be recorded. The intensity measurement with phase changes of 90 degrees in turn can be written as

$$\begin{aligned} I_1(x,y) &= I_0(x,y) \left\{ 1 + b(x,y) \cos [\phi(x,y)] \right\} \\ I_2(x,y) &= I_0(x,y) \left\{ 1 + b(x,y) \cos [\phi(x,y) + \pi/2] \right\} \\ I_3(x,y) &= I_0(x,y) \left\{ 1 + b(x,y) \cos [\phi(x,y) + \pi] \right\} \end{aligned}$$

leading to the phase distribution across the fringe pattern, namely

<sup>1)</sup> Prof. Dr. H.J. Tiziani, Institute of Applied Optics, University of Stuttgart, 7000 Stuttgart 80, FRG

$$\phi(x,y) = \tan^{-1} \frac{2I_2(x,y) - I_1(x,y) - I_3(x,y)}{I_3(x,y) - I_1(x,y)} \quad (2)$$

In addition to the stepped phase shifts with at least three steps the phase shift can vary linearly in time and linearly ramped during the detector integration time. Usually the total integration is the same for each data frame. The detector array will integrate the fringe intensity data over some change in relative phase denoted as  $\Delta$ . One data set of recorded intensity values is given by [15]

$$I_i = \frac{1}{\Delta} \int_{\delta_i - \Delta/2}^{\delta_i + \Delta/2} I_0(x,y) \left\{ 1 + b(x,y) \cos[\phi(x,y) + \delta(t)] \right\} d\delta(t)$$

where  $\phi$  is the wavefront being measured and  $\delta_i$  the average value of the relative phase shift of the  $i$ -th exposure. The integration over a linear phase shift change  $\Delta$  leads to the recorded intensity

$$I_i(x,y) = I_0(x,y) \left\{ 1 + b(x,y) \frac{\sin \pi \Delta/2}{\pi \Delta/2} \cos[\phi(x,y) + \delta_i] \right\}$$

which leads to the so called integrated bucket method. The difference between integrating and stepping the phase is a reduction in the modulation of the interference fringes after detection. For stepped phase shifts ( $\Delta=0$ ) and not integrated, there is no intensity modulation. For the four-bucket technique, four sets of fringe intensities are recorded with

phase shifts of  $\delta_i = -\frac{3\pi}{4}, -\pi/4, \pi/4,$  and  $\frac{3\pi}{4}$ , leading to the phase

$$\phi(x,y) = \tan^{-1} \frac{I_4(x,y) - I_2(x,y)}{I_1(x,y) - I_3(x,y)} \quad (3)$$

To reduce the influence of phase shift errors the 5 step method with 5 phase shifts of  $\pi/2$  is useful.

Digital interferometry is very useful for getting the interferometric data into a computer for the analysis. Computer analysis of interferometric data can be carried out in different ways leading to precise measurements for testing wavefronts of optical surfaces and components. An experi-

A one-dimensional fringe analysis is shown in Figure 2b., the corresponding one-dimensional „microroughness” analysis obtained from the same interference pattern is shown in Figure 2c. The sensitivity obtained is  $\lambda/100$ . For the automatic fringe analysis a CCD line scan camera with 2048 elements or CCD arrays with 256 x 256 elements together with an IBM PC or IBM-AT were used. Alternatively, for some applications with two-dimensional analysis we use a Hamamatsu C 1000 camera. From the fringe pattern stored in a small computer the desired information such as the aberration coefficients or the influence of adjustment errors can be found. Zernike polynomials are found to be appropriate for the study of the wavefront because of their orthogonal properties [3]. Furthermore, the optical transfer function or the point spread function can be obtained.

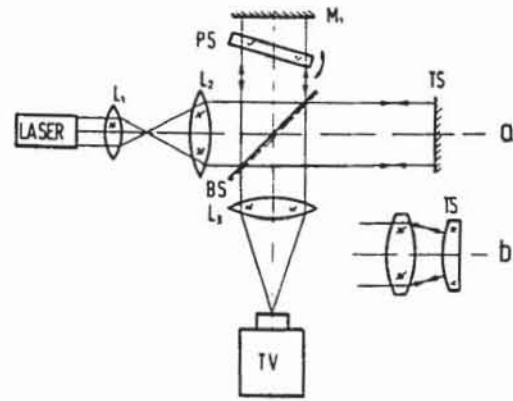


Fig. 1: Twyman-Green interference two beam arrangement

For microprofile measurements, stylus instruments are among the most highly developed means of profiling of precision surfaces. Electron microscopy can be used to produce contour maps and surface profiles of precision surfaces by using two perspective angles.

Interferometric techniques are well suited for microprofile measurements. Two as well as multiple beam interference arrangements with automated fringe analysis can lead to a



Fig. 2a: Interference pattern obtained from a diamond turned spherical surface tested with  $\lambda = 633$  nm.

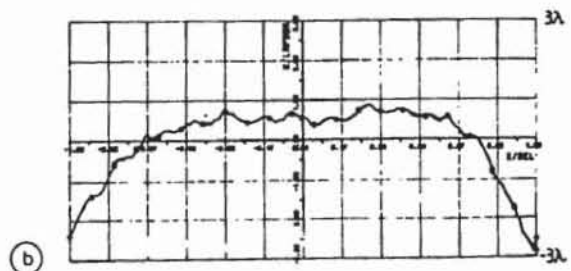


Fig. 2b: One-dimensional fringe analysis of Fig. 2a using 2048 data points.

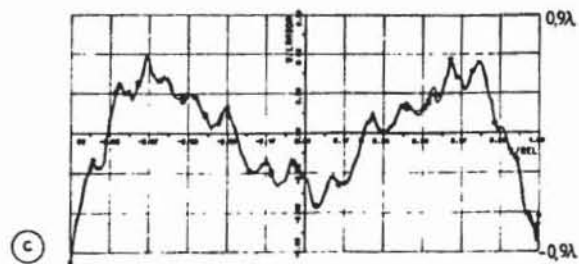


Fig. 2c: Microstructure analysis of Figure 2a.

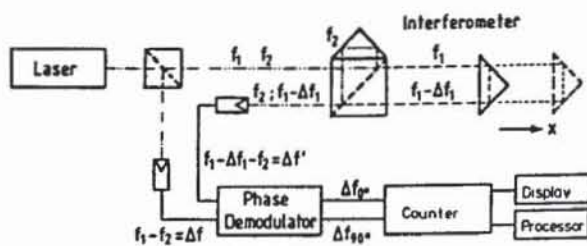


Fig. 3: Principle of heterodyne interference for distance measurement.

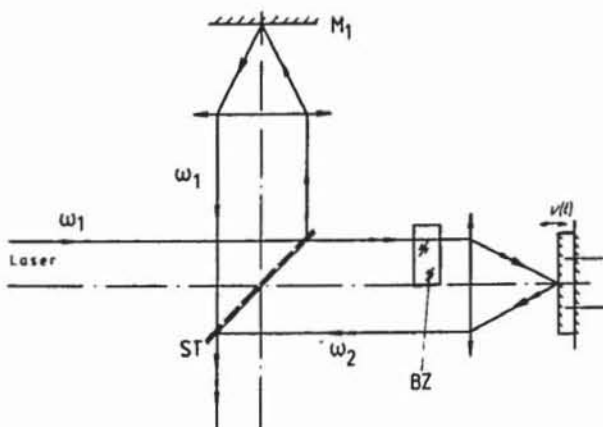


Fig. 4: Principle of heterodyne interference for point by point analysis, BZ = Bragg cell.

resolution of the order of 1 Å as shown by Wyant and co-worker [4]. Recently heterodyne interference arrangements were presented capable of 0,1 Å vertical resolution and a few micrometer lateral resolution [6].

### 3. Application of heterodyne interferometry

In interferometry, phase differences of optical fields are transformed into detectable intensity variations. For two-beam interference, the two light fields are assumed to be

$$A_1 = a_1 \cos(\omega t + \phi_1)$$

$$A_2 = a_2 \cos(\omega t + \phi_2)$$

leading to the intensity

$$I_1 = |A_1 + A_2|^2 = |a_1|^2 + |a_2|^2 + 2a_1 a_2 \cos(\phi_2 - \phi_1) \quad (4)$$

The sensitivity depends mostly on the analysis of the phase difference  $\phi_2 - \phi_1$ . To improve the sensitivity phase shifting techniques are used.

In classical interferometry, phase differences of optical fields are transformed into detectable intensity variations. In two beam heterodyne interferometry the two light fields are assumed to be

$$A_1 = a_1 \cos(\omega_1 t + \phi_1)$$

and

$$A_2 = a_2 \cos \{ \omega_1 t + \Delta\omega t + \phi_2 + \phi(t) \}$$

where  $\Delta\omega$  is proportional to the frequency shift ( $f_2 - f_1$ ) which can be introduced by a Bragg cell or a moving grating or Zeeman splitting. In heterodyne detection by a square-law detector the detector output is

$$I = 2a_1 a_2 \cos(\Delta\omega t + \phi(t) + \phi_2 - \phi_1) \quad (5)$$

where the time varying phase  $\phi(t)$  can be detected. The measurement of the velocity  $v = \frac{dz}{dt}$  (parallel to the optical axis Figure 4.) follows from  $\phi(t) = \frac{2\pi}{\lambda} 2v(t) \cdot t$

For a harmonically oscillating object  $\phi(t) = \frac{4\pi}{\lambda} \rho \cos(\Omega t)$  producing a frequency modulated output signal at the detector with a carrier frequency of  $\Delta\omega/2\pi$  and a frequency and amplitude of modulation  $\Omega$  and  $\rho$  respectively [9]. The signal can be evaluated by well known frequency analysis

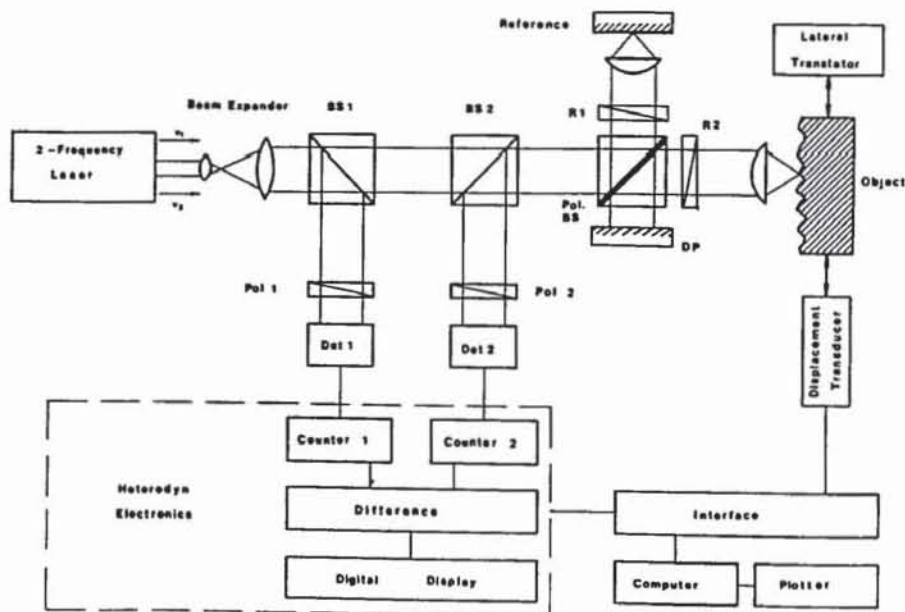


Fig. 5a: Arrangement for microprofile measurement.

techniques. Figure 3. shows schematically a two beam heterodyne interferometer for precise distance measuring where  $\Delta f_1$  is proportional to  $\frac{dz}{dt}$ .

It is basically the concept of the well known HP-interferometer. Figure 4. shows schematically an arrangement for a point by point analysis of a surface by heterodyne interferometry. The microprofile of Figure 5b was obtained by scanning a surface with the heterodyne interference arrangement shown in Figure 5a(Reference 7). The resolution obtained is of the order of an Å.

Figure 6, shows an example of the frequency analysis leading to the velocity at a single point (perpendicular to the surface) of the side wall of a rotating car-tyre obtained with heterodyne interferometry. The arrangement used is shown schematically in Figure 4. For comparison an independent measurement obtained by a microphone is indicated by dotted lines in Figure 6. Close agreement is obtained between the noise detected with a microphone and the noise generated by vibration only.

Heterodyne interferometry will lead to very useful future applications in precision measurements. For the vibration analysis at given points heterodyne interferometry gives not only the amplitude of vibration parallel to the line of sight but also the frequency. Furthermore, it helps for the fringe analysis in holographic interferometry where the fringes are related to the vibration at given points obtained by a heterodyne technique.

By contrast, the laser Doppler velocimeter is used to measure flow velocities of gases and liquids, using the light scattered from small particles suspended in the flowing medium. The speed of optically rough surfaces can be determined by similar methods.

#### 4. Engineering Application of Holographic Interferometry

Holography is a technique by which a wavefront of an object with an optically rough surface is recorded together with a reference wave. The reconstruction in the absence of the object gives the same physical effect as the observation of the original object. Holographic interferometry enables the analysis of static and dynamic displacement of optically rough surfaces to be measured interferometrically. First reports of the method appeared during the mid 1960s and were soon followed by numerous papers describing new applications.

The major applications of holographic interferometry are in measuring mechanical displacement, vibration, strain and deformation. Depending on the application, different techniques were developed. Double exposure, multiple and time average exposure technique were introduced, as well as beam modulation and stroboscopic exposures [10–14]. In addition, fringe localizations together with fringe pattern analyses in three dimensional space have been investigated. By 1970, published material was available predicting the object motion from the fringe pattern. Methods were established to extract vectorial object displacement from the fringes, their parallax and their localization required in their applications. The search for simpler techniques of describing fringes in holographic interferometry initiated various studies on fringe analysis. The theories developed so far simplify the analysis and make it easier for the engineer to understand and apply it. Sometimes, however, they are too difficult to be of practical value for engineering problems, they can be useful for special applications.

In recent years, matrix and tensor calculus have been introduced for fringe analysis, leading to a number of strain analysis techniques. Phase detection has been significantly

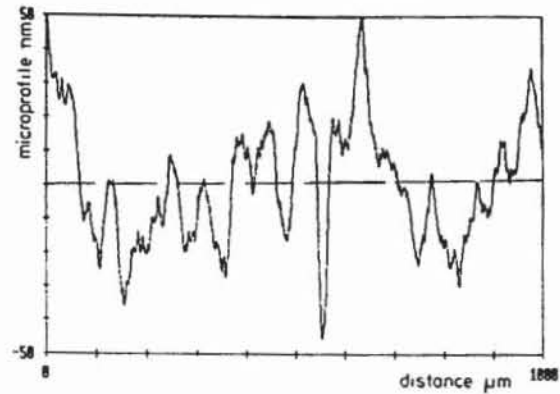


Fig. 5b: Microprofile of a hand polished metal surface with arithmetic mean roughness of  $R_a=0,025 \mu\text{m}$ .

improved to one part in 1000 by heterodyne interferometry [9]. Now at last, holographic interferometry is beginning to show its true potential in structural metrology.

#### 5. Holographic non-destructive testing

The application of holographic techniques to routine inspection of products or components by manufacturers is rather limited. Wide industrial acceptance for non-destructive testing (NDT) was found by testing new and retreated tires. Most commercial aircraft tire manufacturers use the holographic techniques today. There is reason for optimism regarding holographic NDT.

Factors which have led to slow industrial acceptance of the technique include:

- time-consuming wet processing of holograms on silver halide emulsions together with the requirement of high operator skill
- time-consuming processing of the fringe patterns
- relatively fixed sensitivity of holographic interferometry
- requirement of reliable rugged computer controlled lasers easy to field service for CW and dual pulsed holography.

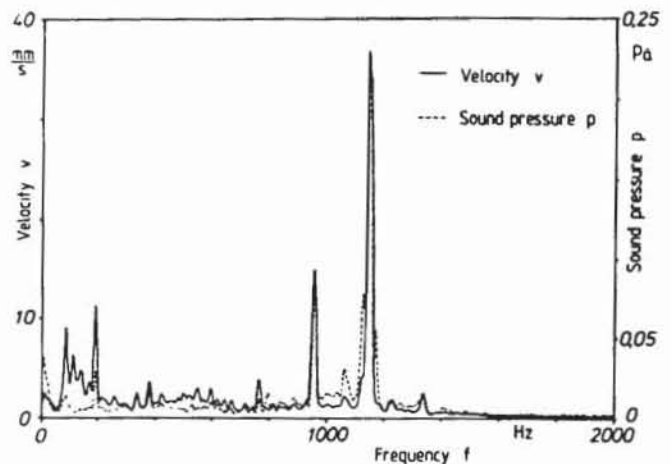


Fig. 6: Comparison of the optical analysis of a rotating car tyre and a microphone placed appropriately. It shows that the airborne sound is due to the structureborne sound.

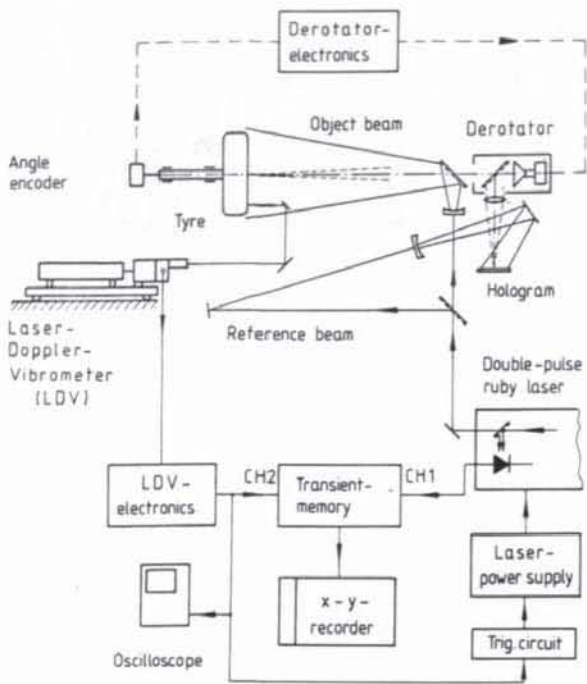


Fig. 7: Holography arrangement for rotating objects.

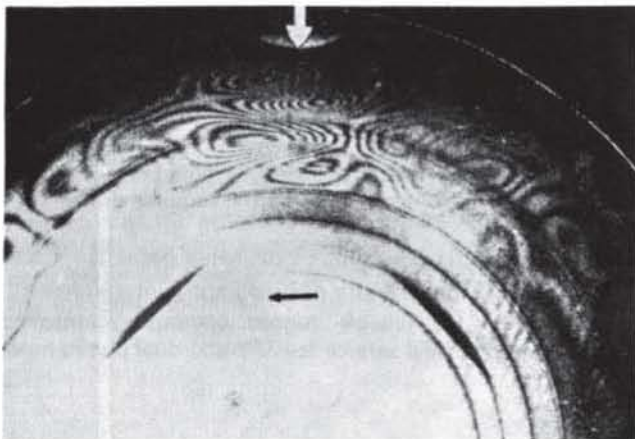


Fig. 8: Fringe pattern of a rotating car tyre, arrow indicates simulated road contact

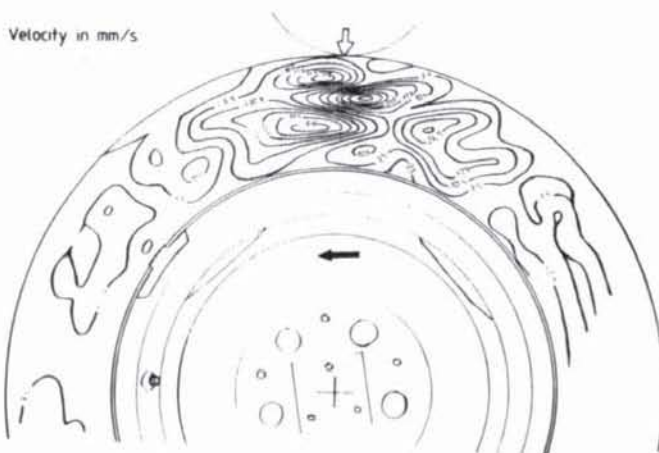


Fig. 9: Fringe pattern analysis of Fig. 8.

There is reason for optimism regarding holographic NDT because many of the above difficulties are and will be taken care of in the near future. New fringe analysis procedures have been introduced and will be further improved. The availability of convenient and reliable photoconductor-thermoplastic cameras allowing exposure, development and viewing of holograms on films or on a reusable plate in a matter of a few seconds has great potential impact on the industrial viability of holographic NDT. Other quasi real time storage materials such as photorefractive electrooptical crystals will be developed.

Research will continue on the application of digital and electronic technology for automated readout and analysis of fringe patterns. Computational methods will be further improved.

Different techniques can be combined with holography to lead to powerful system for NDT. Speckle photography and digital speckle pattern interferometry improve the non-destructive testing. Digital speckle pattern interferometry (DSPI) is a variation of electronic speckle interferometry developed by combining holography and speckle interferometry. In DSPI the speckle patterns are processed digitally, instead of using analog electronics.

## 6. Holographic interferometry of rotating objects

The analysis of deformation, strain and vibration of rotating objects requires unwanted rigid body rotation to be eliminated while preserving the information about the elastic object deformation.

Three methods have been used to carry out holographic interferometry and speckle techniques on rotating objects. These are stroboscopic; rotating plate; and image derotated holographic interferometry.

The stroboscopic method consists in making a hologram of the object while stationary. For the second exposure with strobed light, the rotating object is illuminated, the illumination being at the same angular orientation to the object as for the first exposure.

Rotating-plate holographic interferometry uses the holographic plate fixed to the rotating axis of the subject, but this is not always possible. In addition, the rotating hologram itself will be subject to vibration or rigid body motion, hence complicating fringe analysis is required.

Image derotation is the most promising approach for the study of rotating objects with holographic or speckle techniques [15, 16]. In this method, the image of the rotating object is passed through, or reflected by a prism or mirror rotating at half the rotational speed of the object, thus cancelling out the rotational motion. A Q-switch double-pulsed ruby laser is then used to produce a double-exposure hologram of the rotating object.

An experimental set-up used for image-derotated holographic interferometry is shown in Figure 7. Light from the double pulse ruby laser is divided by a beam splitter and illuminates the object via a second beam splitter. The reflection of the object passes through the derotator prism to interfere with the reference beam on the holographic plate and forms an image-plane hologram. For the alignment it is important that the axis of the derotator is collinear with the rotation axis of the object, otherwise optical-path length differences will produce bias fringes between the two laser pulses. The exact 2:1 ratio between the object and prism speed is achieved by mounting an encoder disk on the drive shaft of the object and relaying its signals to an electronic unit controlling the speed of the servo motor.

In addition, a laser Doppler vibrometer can be used for the vibration analysis at the given point. It can be used as a point of reference for the fringe analysis.

In a research project we have studied the noise of rotating car tyres [16] Figure 7. shows the experimental arrangement with derotator and double pulse laser. Figure 8. shows the fringe pattern obtained by pulse separations of 100 μs at n = 320 min<sup>-1</sup> and a pulse width of 40 ns and Figure 9. the corresponding contour lines of fringes of equal amplitude of vibration.

For noise analysis, a frequency analysis of vibration is required. A heterodyne technique can be used for the analysis of the amplitude and for the frequency of vibration at one or several points. In addition this facilitates fringe analysis in holographic interferometry. The two methods can therefore be used in parallel, the heterodyne technique for the analysis of the vibrations at a given point and the holographic for the analysis of the spatial amplitude distribution of the vibration with reference to the movements at a single point.

### 7. Phase shifting in holographic interferometry

The availability of solid state detector arrays and microprocessors lead to powerful fringe analysis methods in holography. Phase shifting techniques in interferometry can be used. For phase shifting a plane parallel plate can be tilted, alternatively a reference mirror can be mounted on a piezo-electric transducer.

In real-time holographic interferometry a phase shift Ψ is introduced into the reconstructed reference wave leading to a resulting instantaneous irradiance of the hologram. The phase shifting will be described briefly in the double exposure technique where two reference waves are used.

#### Holographic interferometry using two reference beams

##### a) Phase shifting technique in double exposure holography

The use of two reference beams when recording the holograms leads to a simple implementation of the phase-shifting technique for the fringe analysis. The holograms are reconstructed with the two reference waves where one is phaseshifted relative to the other by means of a piezo transducer or by tilting a plane parallel-plate as in two-beam interferometry. Phase shifts of 90 or 120 degrees can be introduced.

For the double exposure technique the first hologram is recorded with the first reference wave shown in Figure 10. The second exposure of the deformed object caused by loads, pressure, temperature variation follows with the slightly tilted second reference wave. The reconstruction of the double exposed hologram (with the two reference waves phaseshifted by steps of π/2 for instance) leads to four wavefronts not counting the four complex conjugate wavefronts. Two are spatially separated due to the tilt of the reference waves, the two other form the interference fringes, namely

$$I = c |U_o|^2 \{ 1 + m \cos [ (\phi - \bar{\phi}) + \psi_K ] \} \quad (6)$$

where  $U_o$  is the reconstructed object wavefront and  $\psi_K$  with  $K = 1, 2, 3$ , are the phase steps,  $(\phi - \bar{\phi})$  the phase difference of the deformed wavefront to be measured. The data are read into the image processor by means of a TV technique (diode arrays). The analysis of the interference pattern is similar to the technique discussed for two beam interferometry. The computer aided evaluation of the data allows a precise analysis of the deformation of the objects

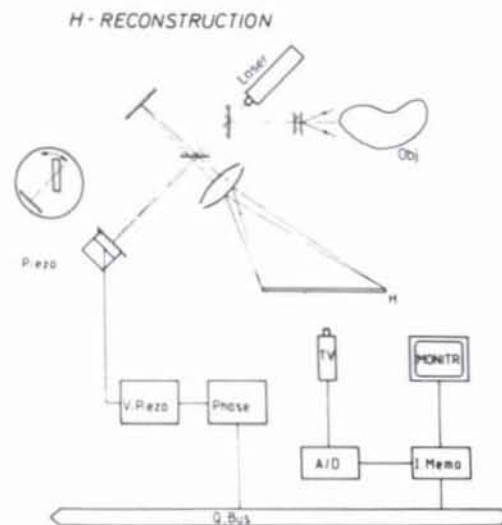


Fig. 10: Arrangement for double exposure holographic technique using two reference beams.

under load. The data can be presented as a 3-D-plot or as contour lines as shown in Figure 11a. and 11b. respectively or as a colour graphic [10-14].

The concept of computer holographic analysis with the appropriate optoelectronic preprocessing assures high accuracy in the evaluation of holographic measurement data. Therefore, the determination of deformation and stress of components can easier be obtained from the holographic deformation data.

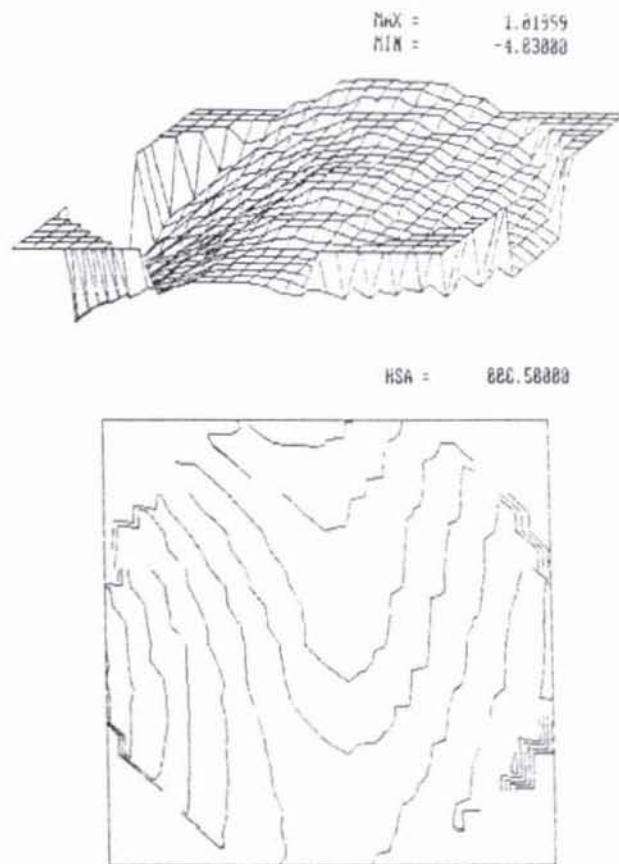


Fig. 11: Result of fringe analysis with two-reference-beam-technique  
11a: 3D-plot.  
11b: contour lines.

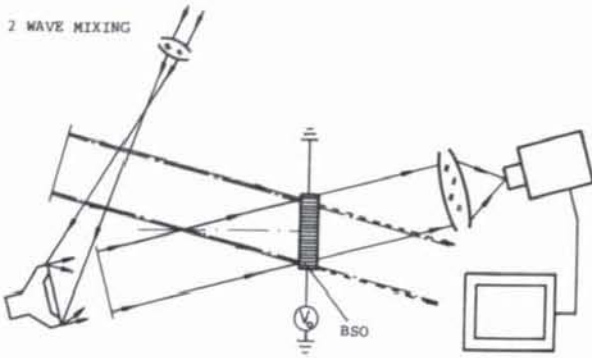


Fig. 12a: Two wave mixing arrangement.

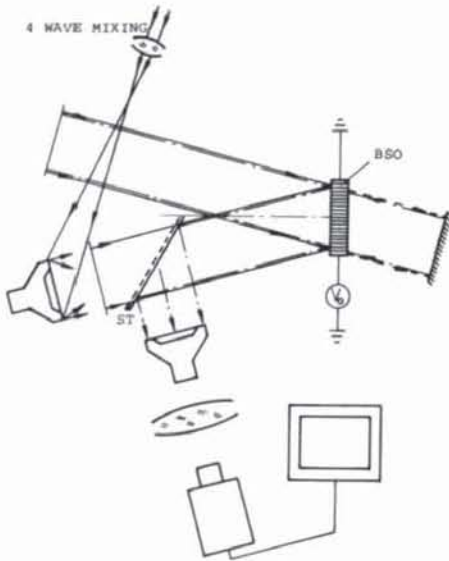


Fig. 12b: Four wave mixing arrangement.

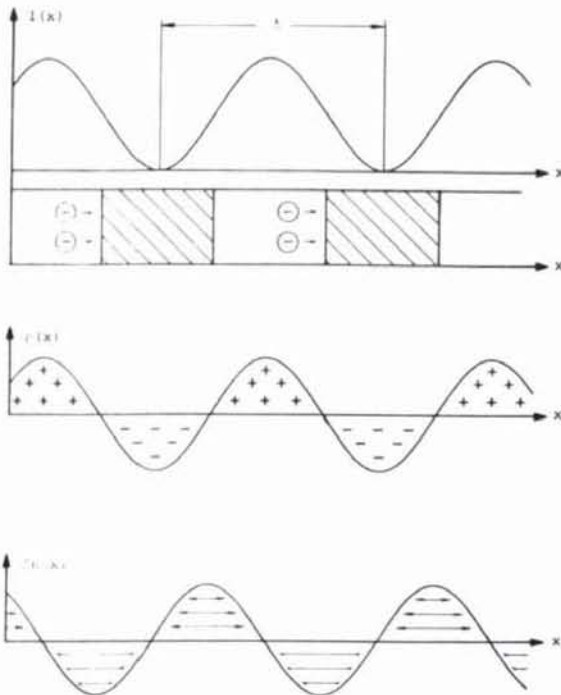


Fig. 13: Principle of the information storage in photorefractive material.

## b) Heterodyne holographic interferometry

The principle was discussed in heterodyne interferometry [9]. The frequency difference of a few hundred KHz can be introduced by a rotating grating when using the direct and diffracted waves or by two acousto-optical modulators arranged in cascade to give opposite frequency shifts. During recording both modulators are driven with 40 MHz. In the reconstruction one is driven with 40,1 MHz leading to a frequency shift of 100 KHz. Scanning the image of the objects with a fringe pattern using a stationary reference and a scanning detector leads to the phase difference  $(\phi - \phi)$ .

To obtain the phase difference in orthogonal directions three detectors are used. The phase differences can be measured with two zero crossing phase meters, which interpolate the phase angle to  $0,1^\circ$ . Heterodyne holographic interferometry requires sophisticated electronic equipment and mechanical scanning of the image by photo-detectors. It is well suited when high sensitivity is required. By contrast the two reference beam phase shifting technique with TV-detection is simpler and requires a videoelectronic data acquisition system.

## 8. Holographic interferometry in real time

The storage media used for holographic interferometry are mainly photographic materials based on silver halide. Alternatives are photoresist, dichromated gelatine, photochromic or thermoplastic materials, or photorefractive electrooptical crystals. Thermoplastic storage material is frequently used in holographic interferometry.

Holographic interferometry is more attractive to the engineer when it can be applied in real time. Photorefractive materials such as lithium niobate ( $\text{LiNbO}_3$ ), potassium niobate ( $\text{KNbO}_3$ ), barium titanate ( $\text{BaTiO}_3$ ), strontium barium niobate (SBN) and bismuth silicon oxide ( $\text{Bi}_{12}\text{SiO}_{20}$ ) are attractive new candidates for real-time optical data processing. Reversible holographic storage was first demonstrated in  $\text{LiNbO}_3$ . More recently,  $\text{BaTiO}_3$ , and  $\text{Bi}_{12}\text{SiO}_{20}$  (BSO) and  $\text{Bi}_{12}\text{GeO}_{20}$  (BGO) were applied for the storage of holograms and speckle patterns [17–27]. Photorefractive crystals can be used for real time metrology using holography in a two or four wave mixing arrangement as shown in Figure 10. We use very often BSO crystals in our laboratory because the BSO is known to be a fast and sensitive material, with a relatively small electro-optic coefficient. By contrast,  $\text{BaTiO}_3$  has larger electro-optic coefficients and is highly efficient, but it responds rather slowly.

One model to describe the charge transport in the photorefractive material is the band transport model assuming that electrons (or holes) are optically excited from filled donor (or acceptor) sites to the conduction (or valence) band where they migrate to dark regions in the crystal by drift or diffusion before recombining into an empty trap. The transported charges result in an ionic space charge grating which is, in general, out of phase with the incident irradiance as shown schematically in Figure 11. The space charge grating is balanced by a periodic space charge electric field modulating the refractive index through the electro-optic effect as indicated in Figure 11. The sensitivity of the BSO is comparable with that of the Kodak 649F emulsion ( $0.3 \text{ mJ/cm}^2$ ) and the information (hologram) can be stored more than 24 hours. Flooding with uniform illumination leads to erasure of the stored information by space charge relaxation. Consequently, reading out with the recording wavelength is destructive.

For holographic interferometry in quasi real-time one hologram of the object to be studied is stored before the

deformation has taken place as shown in two wave mixing (Figure 12a.) or four wave mixing arrangement (Figure 12b.). Immediately after the deformation has taken place a second hologram is stored and reconstructed together with the first one. Interference fringes occur as result of the wavefront modification between the two exposures. Time average exposure recording can be applied for harmonically oscillating objects. Figure 15a. shows an example of an oscillating membrane recorded in the time average. The oscillating frequency was 5,1 kHz and the exposure time less than one second. By contrast the fringe pattern of the same harmonically oscillating membrane obtained with electronic speckle interferometry is shown in Figure 15b. For the analysis of the fringe pattern, TV-techniques and phase shift techniques as described in section 2 can be applied in quasi real-time.

An important application of photorefractive crystals is in the phase conjugation technique where environmental disturbances can be compensated by the reconstruction in an arrangement similar to that shown in Figure 12b.

For contour line holography in quasi real-time a BSO crystal can be used as storage material [12]. There are different ways to form contour fringes that are contours of constant depth. The object can be illuminated with two wavelength simultaneously; illumination with one wavelength but from two directions; or with one wavelength but with a medium of different index surrounding the object. Figure 16. shows the result of quasi real-time 2 wavelength contour line holography using BSO. The separation of two contour lines corresponds to 14  $\mu\text{m}$  depth difference.

For shape and size comparison, for instances, the optical correlation is an alternative to the digital image processing. Furthermore, optical techniques are useful for preprocessing and parallel processing. Optical correlation techniques were not very successful in the past. One of the main reason for the limited application of optical correlation is the occurrence of the speckles, a phenomenon which appears whenever an optically rough surface is illuminated with laser light.

Photorefractive materials can be useful for quasi real-time optical correlation. To avoid most of the speckle noise, the object to be compared or measured can be illuminated with incoherent light.

A light wave based on the variation of the refractive index proportional to the intensity variation over the crystal area, for instance, can be used to convert the incoherent image into a coherent one from where coherent optical correlation can proceed. Some of the spatial light modulator, SLM, use liquid crystals as the electrooptic material and  $\text{Bi}_{12}\text{SiO}_{20}$  (BSO) as the photoconductive material; they are rather expensive and their response time is limited [21]. Other concepts are the microchannel spatial light modulator or the deformable surface spatial light modulator with a limited spatial resolution of 10 lines/mm.

Bulk monocrystalline BSO has useful photoconductive and electrooptical properties. Depending on the local illumination, the crystal will become birefringent [17]. An example of quasi realtime correlation will be described briefly.

For shape comparison in quasi real time an arrangement similar to that of Figure 17. can be used for position invariant correlation. The Fourier spectrum of the object  $O$  and the reference  $R$  illuminated coherently if necessary after incoherent/coherent transformation with  $\lambda_1$  are superposed. The quasi real time reconstruction can be obtained by illuminating the BSO with  $\lambda_2$  as shown schematically

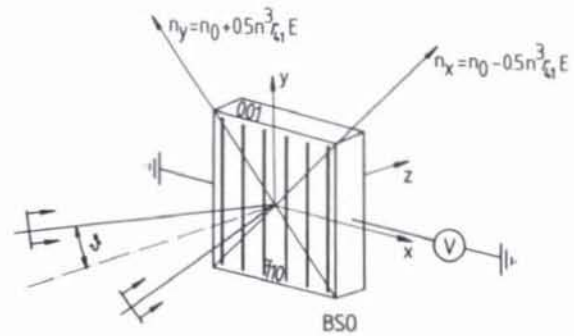


Fig. 14: BSO crystal with applied transversal electric field.



Fig. 15a: Quasi real time fringe pattern obtained in the time average, with BSO, of a harmonically oscillating membrane

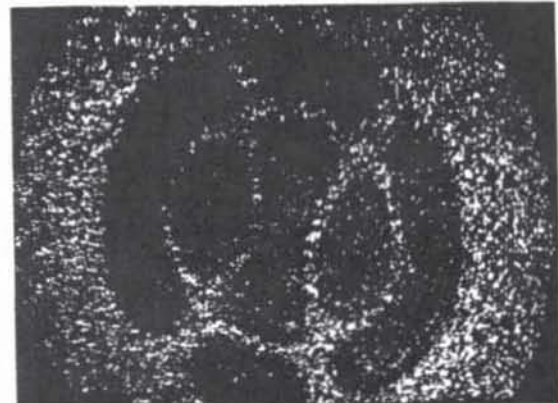


Fig. 15b: Fringe pattern of the harmonically oscillating membrane obtained in the time average with speckle interferometry



Fig. 16: 2 wavelength contour line holography in quasi real time using a BSO crystal as storage material, separation of contour lines 14  $\mu\text{m}$

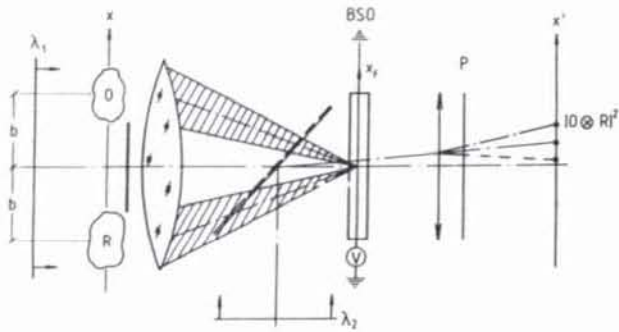


Fig. 17: Arrangement for optical correlation with BSO in quasi real time.

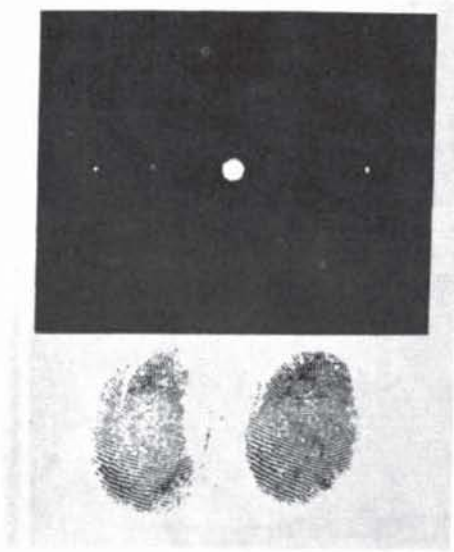


Fig. 18: Result of the correlation of two finger prints.

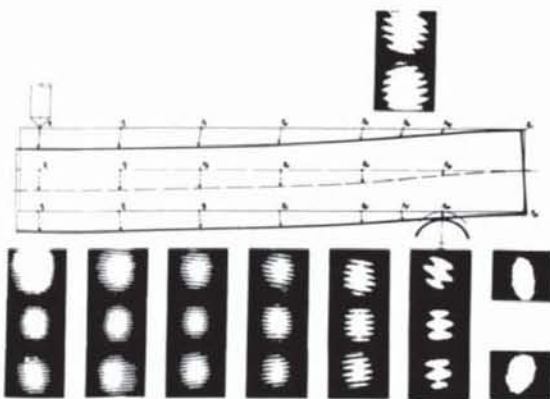


Fig 19: Young's fringes obtained by double exposed speckle photography.

in Figure 17. In the back focal plane of the second lens the cross correlation function of  $R$  and  $O$  is a measure of the similarity between the object  $O$  and the reference  $R$ . An example is shown in Figure 18, where two finger prints are compared. Two peaks of the cross correlation can be seen.

### 9. Application of speckle techniques in metrology

When an optically rough surface is illuminated by a laser, a speckle phenomenon occurs, it is a curious granular appearance. A similar effect occurs in coherent radar and ultrasonic imaging. By an optical rough surface we mean height variation of the order of, or greater than the wavelength of the illumination light. When such a surface is illuminated by a laser beam, the intensity of the scattered light is found to vary randomly with position.

When a laser-illuminated optically rough object undergoes displacement and/or deformation, the speckle in the image field of the object move in addition a change in structure may appear.

#### Speckle Photography

Speckle techniques are a useful tool for determining displacements, vibrations, deformations and contours of a wide range of optically rough surfaces. For speckle photography, an optically rough surface is illuminated with coherent light and photographed either in the image plane, in the Fourier plane or the defocused plane, depending on the application. The recorded image will have a speckled appearance. Exposing the image in photographic film before and after a small object movement (double exposure), pairs of practically identical speckles are recorded. Illuminating the developed double-exposed speckle pattern with a laser beam, Young's fringes are obtained in the Fraunhofer diffraction plane, with a separation inversely proportional to the object displacement. Young's interference fringes occur only if the displaced speckles remain correlated. A point-by-point analysis of the inplane motion of the displacement vector field can be carried out even in the presence of small out-of-plane movements. In Figure 19, Young's fringes of speckle patterns recorded before and after bending a lever are shown. The fringe separation is inversely proportional to the bending.

Speckle photography is by now well understood and can be a useful tool in optical metrology. The limitations are those due to strong deformations (strain), rotation and tilt. For example, deformation and tilt in the presence of translations lead to a limitation of speckle photography due to loss of speckle correlation.

By measurements of the spacing and the direction of the Young's fringe patterns for points on a square-mesh lattice, the two-dimensional strain field can be evaluated. Visual methods for the fringe analysis are time consuming and limited to small sample regions and are heavily dependent on the skill of the operator. For these reasons electrooptical read-out systems with automatic fringe analysis have been studied recently. For good contrast fringes, speckle displacements were obtained to  $0,1 \mu\text{m}$  standard deviation [24].

Bruhn und Felske [25] developed a fast two dimensional Fourier transform analysis of Young's fringes using TV techniques together with image analysis methods in order to construct an automatic fringe analysis system.

#### Electronic speckle pattern interferometric system

For recording interference pattern of diffuse reflecting objects, different names are found in the literature, na-

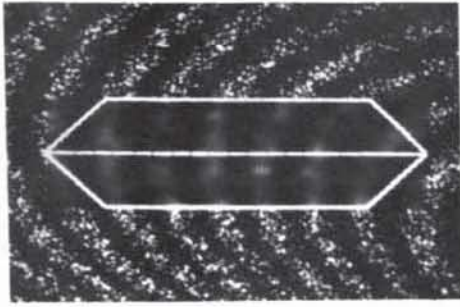


Fig. 20: Speckle interferometry for deformation measurement by double exposure speckle subtraction technique.

mely electronic speckle pattern interferometry (ESPI), TV speckle interferometry, TV holography [22]. The principle of ESPI is similar to a holographic method. It usually combines a specular reference beam as in conventional holography with a superimposed speckled object beam on a vidicon for instance. Cyclically varying fringes occur, corresponding to a path-length change between reference and object beam by  $\lambda$  ( $\lambda$  being the wavelength of the laser). The video signal is processed, high pass filtered, rectified and displayed on the TV monitor. This electronic processing can be considered to correspond to the reconstruction in conventional holography. The image has a speckled appearance, the speckle size is inversely proportional to the aperture of the image forming lens.

On the monitor, fringe pattern occur depending on the subtraction or addition of double-exposed speckle patterns or timeaverage fringes are produced of a harmonically oscillating object. Movements parallel to the line of sight are usually measured. The lateral shifts must be kept smaller than the mean speckle size. For in-plane strain measurements the objects can be illuminated obliquely with two plane waves. Figure 15b. shows a typical time-averaged fringe pattern of an oscillating membrane photographed from the monitor.

A fringe shifting technique can be useful for the automatic fringe analysis of electronic speckle pattern interferometry. The phase in the reference beam can be shifted when recording the speckle pattern by the „double exposure technique“. Figure 20 shows an example of the speckle subtraction technique where a deformation was introduced between the speckle pattern recordings. In addition, three phase shifts of  $\pi/2$  were introduced for the fringe analysis.

In Figure 21. the result of the fringe analysis is shown. The fringes are contour lines of equal deformations.

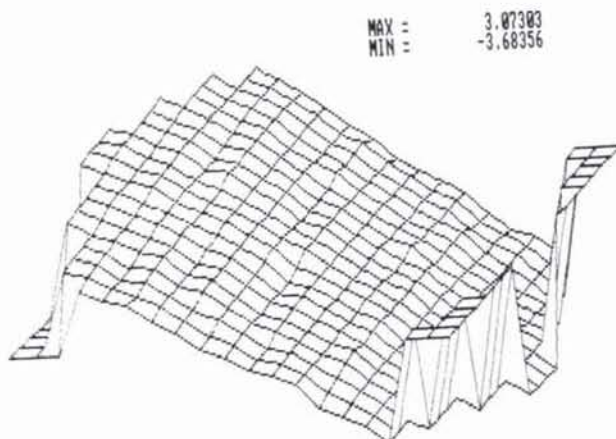


Fig. 21: Fringe analysis of Fig. 20 using phase shift technique.

The storage media used for speckle photography are mainly photographic materials based on silver halide. Alternatives are thermoplastic materials, or photorefractive electrooptical crystals. For quasi real-time speckle photography we use BSO as storage material.

Furthermore, speckle interferometry can be used to investigate fine structure of astronomical objects. Speckle techniques can also be applied for velocity and three-dimensional measurements [26, 27].

Interferometry as well as holographic interferometry and speckle applications are becoming useful tools for industrial applications. The methods can usefully be applied to a considerable variety of engineering measurement problems. Fringe read-out and quantitative analysis of interferometric and holographic data will lead to an improvement of the methods for engineering applications and to the acceptance of laser applications in industry.

#### References

- [1] Takeda, M., Ina, H. and Kobayashi, S., "Fourier transform method for fringe pattern analysis for computer-based topography and interferometry", *JOSA* 72, pp. 156–160. 1982.
- [2] Wyant, J.C., Chapter 12 in *optical shop testing*, ed. Malacara, D., John Wiley and Sons, New York 1978.
- [3] Küchel, F.M., Schmieder, Th. and Tiziani, H.J., "Beitrag zur Verwendung von Zernike-Polynomen bei der automatischen Interferenzstreifenbewertung", *Optik* 65, pp. 123–142. 1983.
- [4] Wyant, J.C., Koliopoulos, C.L. and Bhusban, B. *ASCE Transaction* 27, pp. 101. 1984.
- [5] Greivenkamp, S.E., "Generalized data reduction for heterodyne interferometry", *Opt. Eng.* Vol. 23 (4), pp. 350–352. 1984.
- [6] Huang, C.C., "Optical heterodyne profilometer", *Optical Engineering*, Vol. 23, pp. 365–370. 1984.
- [7] Leonhardt, K., Rippert, K.-H. und Tiziani, H.J., "Verfahren zur optischen Rauheitsmessung und Mikroporfilometrie", *PTB-Bericht* (Ed. K.J. Rosenbruch), PTB, Opt. 19. 1985.
- [8] Dörband, B., Tiziani, H.J., "Auslegung von Kompensations-systemen zur interferometrischen Prüfung asphärischer Flächen", *Optik* 67, pp. 1–20. 1984.
- [9] Dändliker, R., *Progress in Optics*, ed. Wolf, E., North Holland Publ., Amsterdam 1980. Vol. XVII, 1.
- [10] Schumann, W., Dubois, M., "Holographic interferometry", *Springer Ser. Opt. Sci.*, Vol. 16 (Springer, Berlin, Heidelberg 1975).
- [11] Jones, R., Wykes, C., "Holographic and Speckle Interferometry", Cambridge University Press. 1983.
- [12] Pryputniewicz, R.J. and Stetson, "Holographic strain analysis: extension of fringe vector method to include perspective", *Appl. Opt.* 15, pp. 725–728. 1976.
- [13] Breuckmann, B., and Thieme, W., "Computer-Aided Analysis of Holographic Interferograms using the Phase-shift Method", *Appl. Opt.* 24, pp. 2145–2149. 1985.
- [14] Kreis, Th., "Digital holographic interference-phase measurement using the Fourier-transform method", *J. Opt. Soc. Am.* Vol. 3, No 6. 1986
- [15] Fagan, W.P., Beeck, M.A., Kreitlow, H., "Practical application of image derotated holographic interferometry to vibration analysis of rotating components", *SPIE-proceedings* Vo. 36, pp. 260–266. 1980.
- [16] Essers, U., Eberspächer, R., Liedl, W., Litschel, R., Pfister, B., Tiziani, H.J., Zeller, A., "Entwicklungslinien in Kraftfahrzeugtechnik und Straßenverkehr", Verlag TÜV Rheinland, Köln, 1981, 1982.
- [17] Huignard, J.P., Herriau, J.P., Aubourg, P. and Spitz, E., "Phase-conjugate wavefront generation via real-time holography in  $\text{Bi}_{12}\text{SiO}_{20}$  crystals", *Opt. Lett.* 4, pp. 21–23. 1979
- [18] Tiziani, H.J., "Realtime metrology with BSO crystals", *Optica Acta*, Vol. 29, pp. 463–470. 1982.
- [19] Rajbenbach, H., Huignard, J.F. and Loisseaux, B., "Spatial Frequency Dependence of the Energy Transfer in Two-Wave Mixing Experiments with BSO crystals", *Opt. Comm.* 48, pp. 247–252, 1983.
- [20] Küchel, F.M., Tiziani, H.J. "Real-time contour holography using BSO-crystals", *Opt. Comm.* 38, pp. 17–20, 1984.
- [21] Aubourg, P., Huignard, J.P., Hareng, M. & Mullen, R.A., "Liquid crystal light valve using bulk monocrystalline  $\text{Bi}_{12}\text{SiO}_{20}$  as the photoconductive material", *Appl. Opt.*, Vol. 21, pp. 706–3712, 1982.
- [22] Höller, F., Tiziani, H.J., "A spatial light modulator using BSO crystals", *Opt. Comm.* Vol. 58, pp. 20–24. 1986.
- [23] Erf, R.K. (ed.), *Speckle metrology*, Academic Press, New York, 1978.
- [24] Kaufmann, G.H., Ennos, A.E., Gale, B., Pugn, D.J., "An electro-optical read-out system for analysis of speckle photographs" *J. Phys. E. Sci. Instrum.*, Vol. 13, pp. 579–584.
- [25] Bruhn, H., Felske, A., "Schnelle automatische Bildanalyse von Specklegrammen mit Hilfe der Fouriertransformation (FFT) für Spannungsmessungen", *VDI Berichte*, Nr. 309, pp. 13–17. 1981.
- [26] Tiziani, H.J., Leonhardt, K., and Klenk, J., "Real-time displacement and tilt analysis", *Opt. Comm.* Vol. 34, pp. 327–331. 1980.
- [27] Tiziani H.J., Klenk, J., "Vibration analysis by speckle techniques in real time", *Appl. Opt.*, Vol. 20, pp. 1467–1470. 1981.